1-1-2010

Roles of atmospheric and land surface data in dynamic regional downscaling

Deepak K. Ray
Purdue

Roger A. Pielke Sr
Univ. of Colorado

Udaysankar S. Nair
Univ. of Alabama

Devdutta Niyogi
Purdue, climate@purdue.edu

JOURNAL OF GEOPHYSICAL RESEARCH, VOL. 115, D05102, doi:10.1029/2009JD012218, 2010

Roles of atmospheric and land surface data in dynamic regional downscaling

Deepak K. Ray,[1,2] Roger A. Pielke Sr.,[3] Udaysankar S. Nair,[4] and Dev Niyogi[5]

Received 8 April 2009; revised 8 October 2009; accepted 14 October 2009; published 4 March 2010.

[1] In studies dealing with the impact of land use changes on atmospheric processes, a key methodological step is the validation of simulated current conditions. However, regions lacking detailed atmospheric and land use data provide limited information with which to accurately generate control simulations. In this situation, the difference between baseline control simulations and different land use change simulations can be quite different owing to the quality of the atmospheric and land use data sets. Using multiple simulations at the Monteverde cloud forest region of Costa Rica as an example, we show that when a regional climate model is used to study the effect of land use change, it can produce distinctly different results at regional scales, depending on the amount of data available to run the climate simulations. We show that for the specific case of land use change impact studies, the simulation results are very sensitive to the prescribed atmospheric information (e.g., lateral boundary conditions) compared to the land use (surface boundary) information.

Citation: Ray, D. K., R. A. Pielke Sr., U. S. Nair, and D. Niyogi (2010), Roles of atmospheric and land surface data in dynamic regional downscaling, *J. Geophys. Res.*, *115*, D05102, doi:10.1029/2009JD012218.

1. Introduction

[2] Land use change affects atmospheric properties and processes such as surface temperature [*Fall et al.*, 2009], boundary layer processes [*Niyogi et al.*, 1999], radiation balance [*Nair et al.*, 2007], convection [*Pielke*, 2001], mesoscale circulations [*Baidya Roy and Avissar*, 2002], cloud cover and properties [*Ray et al.*, 2003, 2006a], atmospheric dispersion [*Wu et al.*, 2009] and precipitation [*Marshall et al.*, 2004; *Ray et al.*, 2006b; *Pielke et al.*, 2007; *Douglas et al.*, 2009; *Niyogi et al.*, 2010; *Kishtawal et al.*, 2010]. A key methodological step in land use change studies has been to first conduct baseline simulations using the current land use and the initial and lateral boundary conditions. The latter is usually provided from the global or regional reanalysis [e.g., *Mesinger et al.*, 2006; *Ray et al.*, 2009]. The baseline simulations are then evaluated against independent observations. Follow-up simulations are then performed with changed land use but retaining the initial conditions and the atmospheric state for the lateral boundaries of the model domain identical to those of the baseline simulations. The differences (Δ) in model output (meteorological fields) between the simulations are used to quantify the impacts of land use conversion.

[3] The impacts of land use change on regional weather or climate measured through differences have at least two types of uncertainties or errors, besides the uncertainties related to imperfect models: (1) errors due to insufficient atmospheric information (uncertainty in input meteorological data) at the initial state and for the lateral boundary conditions (ε_{Atm}) and (2) errors due to uncertainty in the land information for the current condition (ε_{Land}), such as due to spatially incorrect land use types and/or inaccurate leaf area indices.

[4] Usually, land use change studies have dealt with the impact of converting pristine/forested land to current conditions [e.g., *Marshall et al.*, 2003; *Ray et al.*, 2006a; *Douglas et al.*, 2009] and evaluated by taking differences between meteorological fields such as air temperature, cloud cover, and precipitation between the two model simulations (denoted as F and C in equation (1), respectively). The impact of further land conversion/deforestation was computed in such studies using equation (2) (denoted as C for current and D for further deforestation in equation (2), respectively),

$$\Delta_{F\rightarrow C} = (C - F), \tag{1}$$

$$\Delta_{C\rightarrow D} = (D - C), \tag{2}$$

where the arrows in $\Delta_{F\rightarrow C}$ and $\Delta_{C\rightarrow D}$ show change from F to C and change from C to D, respectively. Differences taken with equations (1) and (2), however, include errors

[1]Department of Forestry and Natural Resources, Purdue University, West Lafayette, Indiana, USA.
[2]Now at the Institute on the Environment, University of Minnesota–Twin Cities, Saint Paul, Minnesota, USA.
[3]Cooperative Institute for Research in Environmental Sciences, University of Colorado at Boulder, Boulder, Colorado, USA.
[4]Earth System Science Center, National Space Science and Technology Center, University of Alabama in Huntsville, Huntsville, Alabama, USA.
[5]Department of Agronomy and Department of Earth and Atmospheric Sciences, Purdue University, West Lafayette, Indiana, USA.

0148-0227/10/2009JD012218$09.00

associated with each simulation (ε), that is, ε_F^T, ε_C^T, and ε_D^T expressed as

$$F = F^T + \varepsilon_F^T, \tag{3}$$

$$C = C^T + \varepsilon_C^T, \tag{4}$$

$$D = D^T + \varepsilon_D^T, \tag{5}$$

where the terms with superscript "T" identify the true state. The errors themselves are made up of an atmospheric (Atm), land use (Land), and model physics part (M); that is,

$$\varepsilon_F^T = \varepsilon_{F,Atm} + \varepsilon_{F,Land} + \varepsilon_{F,M}, \tag{6}$$

$$\varepsilon_C^T = \varepsilon_{C,Atm} + \varepsilon_{C,Land} + \varepsilon_{C,M}, \tag{7}$$

$$\varepsilon_D^T = \varepsilon_{D,Atm} + \varepsilon_{D,Land} + \varepsilon_{D,M}. \tag{8}$$

[5] Since atmospheric information is of course not available for different landscape scenarios, it is generally not possible to quantify the errors in the modeled atmospheric states corresponding to the forested/pristine ($\varepsilon_{F,Atm}$) and deforested/future ($\varepsilon_{D,Atm}$) states. Neither is the accurate prediction of land cover for the future deforested land cover state accurately possible and hence the errors associated with the deforested/future land cover ($\varepsilon_{D,Land}$) are unknown. The forested/pristine land cover can be simulated but generally not validated [e.g., *Ramankutty and Foley*, 1999]. At higher spatial resolutions the spatial and temporal reconstruction of historical land use has been found to be only around 50% accurate even at nonfrontier regions [e.g., *Ray and Pijanowski*, 2010] and thus $\varepsilon_{F,Land}$ are also generally unknown. Evaluation of the errors in model physics was beyond the scope of the current study. Thus, ε_F^T and ε_D^T cannot be estimated. The errors associated with the prescription of the current atmospheric ($\varepsilon_{C,Atm}$) and land use states ($\varepsilon_{C,Land}$) can, however, be estimated [*Ray et al.*, 2009].

[6] Scaling the model error terms $\varepsilon_{F,M}$, $\varepsilon_{C,M}$, and $\varepsilon_{D,M}$ to zero reduces ε_F^T, ε_C^T, and ε_D^T to the estimated error terms ε_F, ε_C, and ε_D, respectively. Then noting the difficulty of estimating ε_F and ε_D, substituting equations (3)–(5) into equations (1) and (2), and rewriting gives

$$\Delta_{F\to C} = \Delta_{F\to C}^T + \varepsilon_C - \overset{0}{\not\varepsilon}_F, \tag{9}$$

$$\Delta_{C\to D} = \Delta_{C\to D}^T + \overset{0}{\not\varepsilon}_D - \varepsilon_C, \tag{10}$$

where Δ^T denotes the accurate estimation of land use change impacts. Note that less accurate impact assessments due to land use changes are more likely to occur in regions with sparse atmospheric and land cover data and where the impacts of ε_C are likely to be larger. Such regions could for instance include areas where (1) regular radiosonde data are not available and (2) good quality land use maps are not available.

[7] The error term ε_C is unknown even when reviewing results from previous studies over different regions [e.g., *Pielke et al.*, 2007]. Moreover, there is confusion regarding whether accurate land use or accurate atmospheric information is more important for improving baseline simulations. Recently, *Ray et al.* [2009] showed that $\varepsilon_{C,Atm}$ were generally reduced when special radiosondes or additional meteorological products are assimilated over data sparse regions when conducting simulations using a type 1 dynamical-downscaling approach. Type 1 dynamic downscaling refers to those simulations that still retain significant information on their initial conditions and also when real world observed data are assimilated during the model integration. Type 2 downscaling, in contrast, refers to those regional model runs where the initial conditions have been forgotten but the simulations are still dependent on the lateral and bottom boundary conditions. The value-added (skill) of type 1 must be equal to or greater than type 2 since the insertion of initial conditions provides a real-world constraint to the accuracy of the regional model. In the type 1 approach as defined by *Castro et al.* [2005], not only initial memory conditions are used but also the model variables are continuously updated using data assimilation from large-scale models such as the National Centers for Environmental Prediction (NCEP) reanalysis [*Kalnay et al.*, 1996]. Other studies [e.g., *Alfieri et al.*, 2007; *Ge et al.*, 2007; *Alapaty et al.*, 2008] have demonstrated that $\varepsilon_{C,Land}$ can be reduced when updated satellite-derived land use information is assimilated in modeling the current conditions.

[8] *Ray et al.* [2009], however, showed that over the Monteverde region of Costa Rica $\varepsilon_{C,Atm}$ was more than an order of magnitude larger than $\varepsilon_{C,Land}$ using type 1 dynamical downscaling in which data assimilation is used during the model integration. They, however, did not investigate the importance of the $\varepsilon_{C,Atm}$ and/or $\varepsilon_{C,Land}$ terms by comparing them to the signal being measured; that is, in equations (11)–(14),

$$\varepsilon_{C,Atm} \approx \Delta_{F\to C}, \tag{11}$$

$$\varepsilon_{C,Land} \approx \Delta_{F\to C}, \tag{12}$$

$$\varepsilon_{C,Atm} \approx \Delta_{C\to D}, \tag{13}$$

$$\varepsilon_{C,Land} \approx \Delta_{C\to D}. \tag{14}$$

[9] This estimation becomes important because if either $\varepsilon_{C,Atm}$, $\varepsilon_{C,Land}$ or both are comparable to change impacts themselves then previous land cover change impact studies may have substantially underestimated or overestimated the impacts on the atmospheric condition simply because of $\varepsilon_{C,Atm}$, $\varepsilon_{C,Land}$, or both. These errors would be potentially larger over data sparse regions and are the subject of the current investigation. Our working hypothesis is that the error terms in the left-hand side of any of the

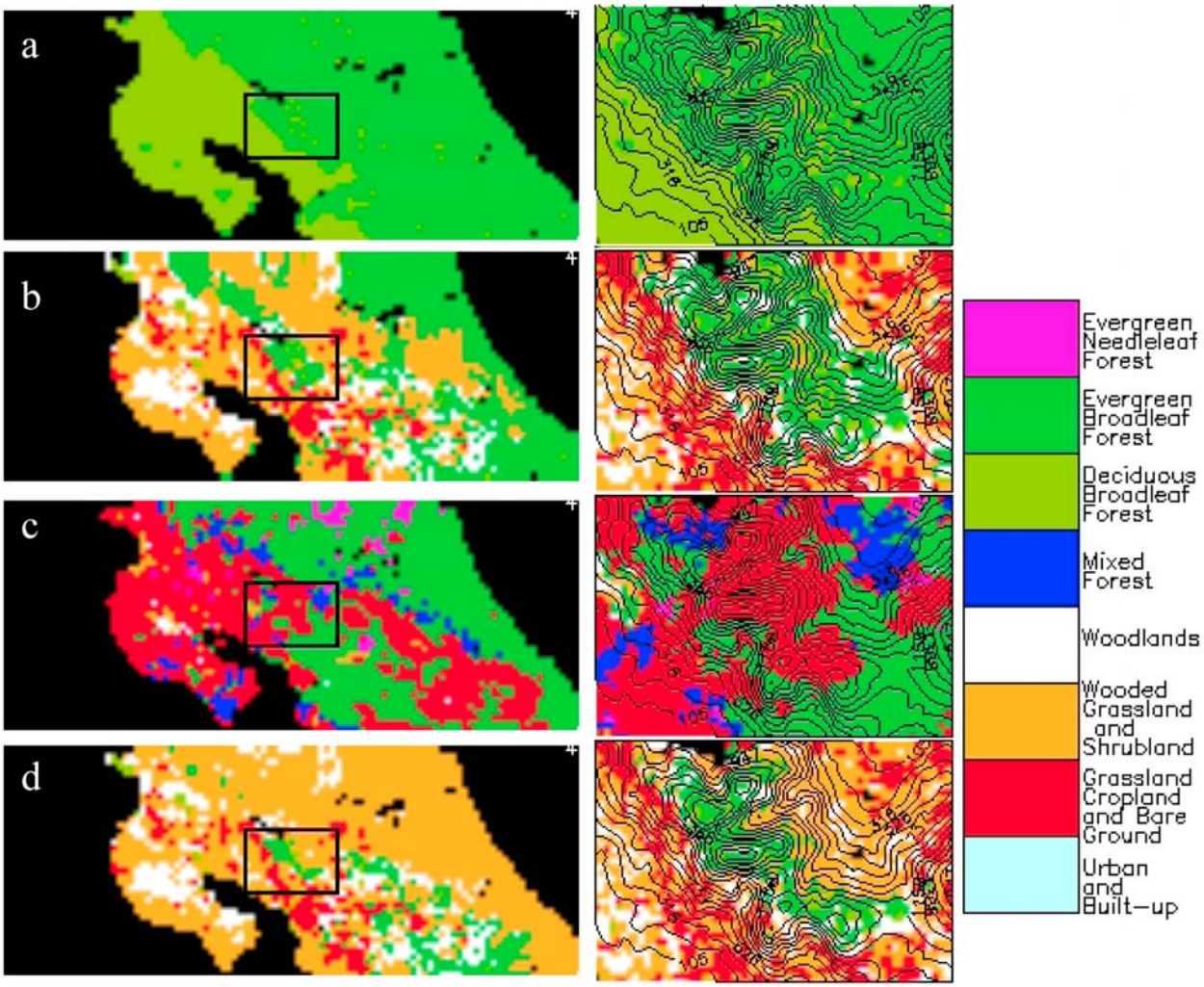

Figure 1. Land use associated with the experiments: (a) forested condition, (b) updated current land use satellite-derived data and expert corrections, (c) model default land use for the current condition, and (d) future deforested scenario. Deforestation was assumed to proceed up to 1000 and 1400 m on the Caribbean and Pacific slopes of the mountains, following *Ray et al.* [2006a]. The left maps are for the outer coarser grid, and the black rectangles in them denote the location of the higher-resolution grid, which is shown in full resolution on the right.

equations (11)–(14) might be large and even similar in magnitude to the land use change impacts being simulated (i.e., right-hand side of equations (11)–(14)).

[10] Note that $\varepsilon_{C,Atm}$ is also likely to occur when a regional climate model (RCM) is used to dynamically downscale current and future scenarios from a global climate model (GCM) (type 2 downscaling in which the initial memory is lost). *Castro et al.* [2005], for example, showed that dynamical downscaling using a RCM does not increase value beyond that of a GCM. Further, at a regional scale, GCM-simulated temperature and precipitation have frequently been found to be inconsistent with current observations (i.e., ε_C are often large). In hydrological studies where large uncertainty in hydrographs result from ε_C in precipitation, the observed precipitation is often scaled by the bias between observations and GCM simulation for the current climate and this bias is used to correct future GCM predictions [*Chiew and McMahon*, 2002; *Tucci et al.*, 2003; *Scibek and Allen*, 2006]. As an analog, the RCM $\varepsilon_{C,Atm}$ could provide an estimate of likely inaccuracies from dynamically downscaling RCM using GCM-simulated current and future scenarios and this Δ could be useful for societal applications as well as for improving the model simulations/predictions [*Visbeck*, 2008].

2. Study Location, Data, and Methodology

[11] To evaluate the errors stated in equations (11)–(14), we performed seven, 14 day (1–14 March 2003) continuous model integrations using the Regional Atmospheric Modeling System (RAMS) [*Pielke et al.*, 1992] over the study region centered on the Monteverde cloud forest (10.25°N, 84.7°W) in Costa Rica (Figure 1). The study region was originally covered with tropical wet and moist forests, but by 1992 the forest cover lowland of Costa Rica was reduced to 18% of the area of the original forest cover. The recent

Table 1. Experiments[a]

Experiment Acronym	Special Radiosondes	Updated Land Cover	Comment
			$\varepsilon_{C,Atm}$ Evaluation
C_SPECIAL_ATM	Y	Y	Current conditions simulated using 86 special rawinsonde in addition to UCAR data sets; updated land cover; MODIS observed LAI
C_STANDARD_ATM	N	Y	Current conditions simulated without special rawinsondes and only using UCAR data sets; updated land cover; MODIS observed LAI
F_STANDARD	N	-	Forest conditions simulated without special rawinsondes and only using UCAR data sets; MODIS observed LAI from current forests
F_SPECIAL	Y	-	Forest conditions simulated using 86 special rawinsondes in addition to UCAR data sets; MODIS observed LAI from current forests
D_STANDARD	N	-	Deforested conditions simulated without special rawinsondes and only using UCAR data sets; MODIS observed LAI from current forests and nonforest locations
D_SPECIAL	Y	-	Deforested conditions simulated with 86 special rawinsondes in addition to UCAR data sets; MODIS observed LAI from current forest and nonforest locations
			$\varepsilon_{C,Land}$ Evaluation
C_SPECIAL_ATM	Y	Y	Same as above
C_STANDARD_LU	Y	N	Current conditions simulated using 86 special rawinsonde in addition to UCAR data sets; model default land cover information
F_SPECIAL	Y	-	Same as above
D_SPECIAL	Y	-	Same as above

[a]UCAR, University Corporation for Atmospheric Research; MODIS, Moderate Resolution Imaging Spectroradiometer; LAI, leaf area index.

average annual deforestation rate is 4.2% owing to the relative ease of clearing land in the lowlands and drier Pacific slopes [*Ray et al.*, 2006a]. Much of the Pacific slopes of the Cordillera de Tilarán, and the Cordillera de Guanacaste were deforested earlier. Pre-Columbian inhabitants lived and farmed (with slash-and-burn techniques) in all but the wettest habitats (R. O. Lawton, personal communication, 2009), but accurate maps of the historical land cover and changes are not available; that is, $\varepsilon_{F,Land}$ cannot be estimated as noted earlier with certainty. The models were run with three land use conditions: pristine/forested (Figure 1a), current (Figures 1b and 1c), and future/deforested (Figure 1d) conditions using standard and special atmospheric data sets to capture $\varepsilon_{C,Atm}$ leading to six models. Thus the experiment setup testing $\varepsilon_{C,Atm}$ is a type 1 downscaling but since type 2 downscaling is necessarily less accurate than type 1, the results also apply to that level of downscaling. One additional simulation was conducted using model default land use to capture $\varepsilon_{C,Land}$ (Figure 1c).

[12] The cloud forests of Monteverde, Costa Rica, rely on horizontal precipitation [*Ray et al.*, 2006a] from clouds (i.e., the cloud base regularly intersects the topography and immerses the forest with cloud water) along steep topographic gradients. This cloud immersion occurs because the consistent northeasterly airflow associated with the trade winds from the Caribbean Sea encounters the central mountain ranges and is forced to orographic lift, leading to condensation. This creates a unique environment that in turn is responsible for the enormous biodiversity found here [*Pounds et al.*, 1999; *Lawton et al.*, 2001]; the surface boundary forcing associated with orographic lifting is thus likely to be strong. Prior research [e.g., *Lawton et al.*, 2001; *Nair et al.*, 2003; *Ray et al.*, 2006a] found that land use change in the upwind lowland areas leads to increased cloud base height reducing horizontal precipitation. Therefore $\varepsilon_{C,Atm}$ (in equations (11) and (13)) was also evaluated for the differences in cloud base height between simulations C_SPECIAL_ATM and C_STANDARD_ATM (Table 1) in addition to assessing the precipitation and surface temperature differences. This can be represented as

$$\varepsilon_{C,Atm} = C_{Atm} - C^{T}_{Atm} \Rightarrow \varepsilon_{C,Atm} = \sum_{comparisons} \cdot (\text{C\_STANDARD\_ATM}_{\text{weather}} - \text{C\_SPECIAL\_ATM}_{\text{weather}}). \quad (15)$$

[13] The comparison of error $\varepsilon_{C,Atm}$ with $\Delta_{F\rightarrow C}$ (equation (11)) was then estimated by comparing $\varepsilon_{C,Atm}$ with the difference between C_STANDARD and F_STANDARD (Table 1), the standard runs that are generally expected. Similarly, the comparison $\varepsilon_{C,Atm}$ with $\Delta_{C\rightarrow D}$ was done by comparing $\varepsilon_{C,Atm}$ with the difference in meteorological variables between D_STANDARD and C_STANDARD_ATM (Table 1).

[14] All the "SPECIAL_ATM" runs were identical to the "STANDARD" simulations with the exception that they utilized 86 special radiosonde observations that were collected during a special field campaign called the Land Use Cloud Interaction Experiment (LUCIE) [*Ray et al.*, 2009], in addition to meteorology provided by the 1° NCEP reanalysis [*Kalnay et al.*, 1996], and the upper air and surface observations from the University Corporation for Atmospheric Research (UCAR) used in the "STANDARD" simulations. Barnes objective analysis using the special radiosonde observations provided additional real world constraints to the "SPECIAL_ATM" simulations. The "STANDARD" simulations were thus similar to what would generally be used by researchers at regions devoid of special radiosonde launches. The special radiosondes were launched at 3 h interval over paired forested and deforested sites from 0600 local time (LT) to 1800 LT. While radiosondes were not launched over the mountains note that orographic uplift was experienced by the radiosondes and sampling over the mountains thus occurred.

Table 2. Average Values Associated With the Experiments[a]

Experiment Acronym	RMSE Precipitation at 92 Rain Gauge Locations (mm)	Average Precipitation at 92 Rain Gauge Locations (mm)	Outer Domain Total Average Precipitation (mm)	Inner Domain Total Average Precipitation (mm)	Inner Domain 2 m Air Temperature at 1400 LT (°C)	Inner Domain Cloud Base Heights at 1400 LT (m)
F_SPECIAL	NA	21.6	41.7	104.9	17.2	1810.6
F_STANDARD	NA	22.3	31.6	29.1	20.6	1939.3
C_SPECIAL_ATM	26.8	20.4	41.9	99.9	18.7	1978.2
C_STANDARD_ATM	35.1	26.0	33.3	46.1	23.0	2389.8
D_SPECIAL	NA	18.2	41.7	90.9	19.1	2079.2
D_STANDARD	NA	31.7	35.7	53.1	23.4	2450.0
C_STANDARD_LU	29.8	20.4	40.7	85.7	19.0	2126.4

[a]NA stands for "not applicable," which refers to the fact that the forest and deforested scenario simulation cannot be validated against rain gauge measurements.

[15] Changes in the error fields from updated land cover information ($\varepsilon_{C,Land}$) were computed by taking the difference between C_STANDARD_LU and C_SPECIAL_ATM (Table 1) and then compared to the difference in meteorological variables between C_STANDARD_LU and F_SPECIAL (i.e., $\Delta_{F\rightarrow C}$ in equation (12)) and to the difference in meteorological variables between D_SPECIAL and C_STANDARD_LU (i.e., $\Delta_{C\rightarrow D}$ of equation (14)). C_SPECIAL_ATM had satellite-derived updated land cover [*Hansen et al.*, 2000] (Figure 1b), whereas C_STANDARD_LU had model default land cover information (Figure 1c). All the $\varepsilon_{C,Land}$ comparison simulations utilized special atmospheric information, so the only difference was in the land cover information in the C_STANDARD_LU simulation.

[16] All the simulations had identical two telescopic nested grid configurations (Figure 1) with 4 km and 1 km grid spacing for the outer and inner nested grids, respectively. In the vertical, a stretched grid that varied from 20 m near the surface to 750 m higher up was used with the top at 24 km. We used a hybrid grid system in the vertical with terrain following sigma z coordinates at lower atmospheric levels blended to isentropic coordinates at 6 km. The lateral boundaries were nudged with an exponentially decreasing nudging strength and with a time scale of 900 s along five grid points. Model runs without interior nudging are not directly influenced by the landscape effect on the radiosondes. However, even for this situation the lateral boundary conditions, of course, are influenced by the current landscape from outside the model domain. Because of the fine grid spacing, microphysical processes were explicitly represented and the atmospheric radiative transfer scheme of *Harrington and Olsson* [2001] was used. A deformation scheme was used to represent horizontal diffusion, while the vertical diffusion was parameterized using the *Mellor and Yamada* [1982] scheme. The soil layer depth was prescribed as 2.5 m and was spatially heterogeneous [*Food and Agriculture Organization*, 1971]. Following *Ray et al.* [2006a], the initial soil saturation prescribed in the simulations varied from the observed values of 0.1 at the surface, 0.2 at 50 cm depth, to 0.3 at 1.0 m depth and linearly increased to 0.8 at 2.5 m soil depth. This soil moisture profile was prescribed for the forested, current, and deforested simulation and is based on observations from the time period of the model simulation. Our analysis of soil moisture from forested and pasture sites showed that they both had a nearly similar soil moisture profile (upper half meter). The profile of deeper soil moisture was from field observations that showed stream flows at half meter depths or lower in this region. Pasture grasses with shallow roots were found generally stressed over the model domain whereas trees had green leaves implying access to deeper soil moisture. On the basis of these sets of observations, the soil moisture was increased to higher values at greater depths (where we did not have any measurements). Sea surface temperature was prescribed following the Moderate Resolution Imaging Spectroradiometer (MODIS) overpass and had a regional average value of 300 K.

3. Results

3.1. Accuracy of the Current Models

[17] The simulations with special radiosondes and updated land cover information are expected to have reduced simulation errors (i.e., $\varepsilon_{C,Atm}$ and $\varepsilon_{C,Land}$, respectively) as compared to the control/standard. Using root mean square error (RMSE) statistics,

$$RMSE = \sqrt{\frac{\sum_{i=1}^{n} (O^i - S^i)^2}{n}}, \tag{16}$$

where O^i and S^i are the observed and model-simulated precipitation, respectively, precipitation comparisons at 92 locations over the entire outer simulation domain were conducted. The total observed precipitation was 542.6 mm for these stations. C_SPECIAL_ATM had a RMSE of 26.8 mm whereas C_STANDARD_ATM had a larger RMSE of 35.1 mm (Table 2) for the simulated time period clearly showing the reduction in precipitation simulation errors as a result of including special radiosondes in the simulations, as expected. Thus, simulations not utilizing special radiosondes at this location and over the time period simulated would get an extra RMSE (i.e., extra $\varepsilon_{C,Atm}$) of 8.3 mm. Indeed, this number will vary depending on the number of special radiosondes used and true differences are of course not possible to estimate; that is, we can only get better estimates of $\Delta^T_{F\rightarrow C}$ and $\Delta^T_{C\rightarrow D}$ and denoted them as $\Delta^*_{F\rightarrow C}$ and $\Delta^*_{C\rightarrow D}$, respectively, in the remainder of this manuscript.

[18] To eliminate the possibility that owing to the chaotic nature of weather, this 2 week period produced the differences in RMSE between the C_SPECIAL_ATM and C_STANDARD_ATM simulations, we first determined the number of days either simulation had lower RMSE. We found that C_SPECIAL_ATM had a lower RMSE on 67% of the days whereas C_STANDARD_ATM had a

Table 3. Estimated $\varepsilon_{C,Atm}$, $\Delta_{F\rightarrow C}$, $\Delta_{C\rightarrow D}$, $\Delta^*_{F\rightarrow C}$, and $\Delta^*_{C\rightarrow D}$

Variable	$\varepsilon_{C,Atm}$	$\Delta_{F\rightarrow C}$	$\Delta^*_{F\rightarrow C}$	$\Delta_{C\rightarrow D}$	$\Delta^*_{C\rightarrow D}$
Averaged Over Remote Inner Domain					
Total precipitation (mm)	−53.8	17.0	−5.0	7.0	−9.0
2 m air temperature (°C), 1400 LT	4.3	2.4	1.5	0.4	0.4
2 m air temperature (°C), 1500 LT	4.1	2.1	1.4	0.4	0.5
2 m air temperature (°C), 1600 LT	3.8	1.8	1.1	0.3	0.5
Cloud base height (m), 1400 LT	411.6	450.4	167.6	60.2	101.0
Cloud base height (m), 1500 LT	449.2	249.0	120.6	128.1	163.1
Cloud base height (m), 1600 LT	207.4	151.9	181.8	185.3	156.9
Averaged Over Remnant Forest Locations					
Total precipitation (mm)	−118.4	28.8	4.7	19.6	−23.6
2 m air temperature (°C), 1400 LT	2.9	0.3	0.2	0.4	0.2
2 m air temperature (°C), 1500 LT	2.7	0.3	0.2	0.4	0.2
2 m air temperature (°C), 1600 LT	2.4	0.1	0.0	0.3	0.2
Cloud base height (m), 1400 LT	751.0	461.0	40.9	97.8	163.1
Cloud base height (m), 1500 LT	777.7	320.5	96.0	109.2	251.1
Cloud base height (m), 1600 LT	534.3	188.2	59.1	180.4	258.6
Averaged Over Deforested Locations					
Total precipitation (mm)	−41.8	14.9	−6.9	4.7	−6.3
2 m air temperature (°C), 1400 LT	4.6	2.9	1.8	0.4	0.5
2 m air temperature (°C), 1500 LT	4.3	2.5	1.7	0.4	0.5
2 m air temperature (°C), 1600 LT	4.1	2.2	1.3	0.4	0.5
Cloud base height (m), 1400 LT	354.7	447.4	184.6	52.5	92.2
Cloud base height (m), 1500 LT	382.2	236.3	129.2	133.5	146.7
Cloud base height (m), 1600 LT	152.2	132.6	205.4	189.9	129.9

lower RMSE for the remaining 33% of the days. Second, we also divided the simulation period into two halves and computed the RMSE for each half to determine whether results were consistent. We found that in the first half, the errors were lower for both the simulations compared to the second half. C_SPECIAL_ATM, however, had a lower RMSE than C_STANDARD_ATM for both periods, implying that this was not an artifact of weather events. The RMSE values were 11.1 mm and 15.8 mm for the first and second half for C_SPECIAL_ATM and 14.7 mm and 23.3 mm for C_STANDARD_ATM, that is, consistent with higher RMSE values for the "STANDARD" simulations.

[19] C_STANDARD_LU (simulation with model default land cover but special radiosondes) had RMSE of 29.8 mm (Table 2), which in comparison to the error of C_SPECIAL_ATM is slightly higher but it is considerably less than C_STANDARD_ATM. This suggests that uncertainties in the atmospheric information impact the simulations more than the uncertainties in the land cover (for our experimental setup).

[20] The average total precipitation difference between C_STANDARD_ATM and C_SPECIAL_ATM at the 92 observation locations was 5.5 mm (27.5% difference); that is, simulations with standard atmospheric data sets overestimated precipitation by 5.5 mm on average. The average $\Delta_{F\rightarrow C}$ and $\Delta_{C\rightarrow D}$ were 3.7 mm and 5.7 mm, respectively, implying deforestation increased precipitation (contrary to expectation here) and further deforestation up to a certain point could create mesoscale heterogeneities which would further increase precipitation, again contrary to expectation at this study site [see *Lawton et al.*, 2001; *Nair et al.*, 2003; *Ray et al.*, 2006a]. Note that other studies such as those in the Sahel have reported an opposite effect [*Taylor and Ellis*, 2006], where the higher sensible heat flux expected in a deforested environment forces faster, deeper boundary layer growth, making it more likely, not less, that deep convection will occur when there is a larger-scale source of water vapor [*Niyogi et al.*, 2002]. This results in more precipitation. *Ray et al.* [2003], in another dry region of southwestern Australia, found fewer cumulus clouds forming climatologically over regions without vegetation cover in the dry season. Differences between simulations utilizing special radiosondes, that is, $\Delta^*_{F\rightarrow C}$ and $\Delta^*_{C\rightarrow D}$, were −1.2 mm and −2.2 mm. Both these are consistent with general expectations at this study site but opposite to the simulation results that used standard atmospheric information showing that utilizing or not utilizing special radiosondes can completely change results.

[21] The average total precipitation difference between C_STANDARD_LU and C_SPECIAL_ATM at the 92 observation locations was −0.05 mm, which is insignificant compared to the difference due to atmospheric information. Average $\Delta_{F\rightarrow C}$ and $\Delta_{C\rightarrow D}$ (i.e., C_STANDARD_LU – F_SPECIAL and D_SPECIAL – C_STANDARD_LU, respectively) were −1.2 mm and −2.2 mm, respectively. Again these results are comparable to $\Delta^*_{F\rightarrow C}$ and $\Delta^*_{C\rightarrow D}$ which shows that utilization of the model default current land cover would have provided similar results at these 92 validation locations.

3.2. Land Use Change Impacts on Meteorological Variables Compared With Differences Between Current "STANDARD" and "SPECIAL" Simulations

[22] Models are typically used to simulate the meteorological impacts of land use changes over remote regions that are presumed sensitive to meteorological changes due to the land use changes. The inner model domain in this study is one such region. The lack of detailed atmospheric and land cover information could result in uncertainty in the simulated meteorological fields from both the errors in input atmospheric ($\varepsilon_{C,Atm}$) and land use ($\varepsilon_{C,Land}$) information. In sections 3.2.1–3.2.3 we discuss the magnitude of these errors and compare them with the meteorological impacts due to land use changes. Large errors could lead to incorrect conclusions regarding the impacts of land use changes on the meteorology.

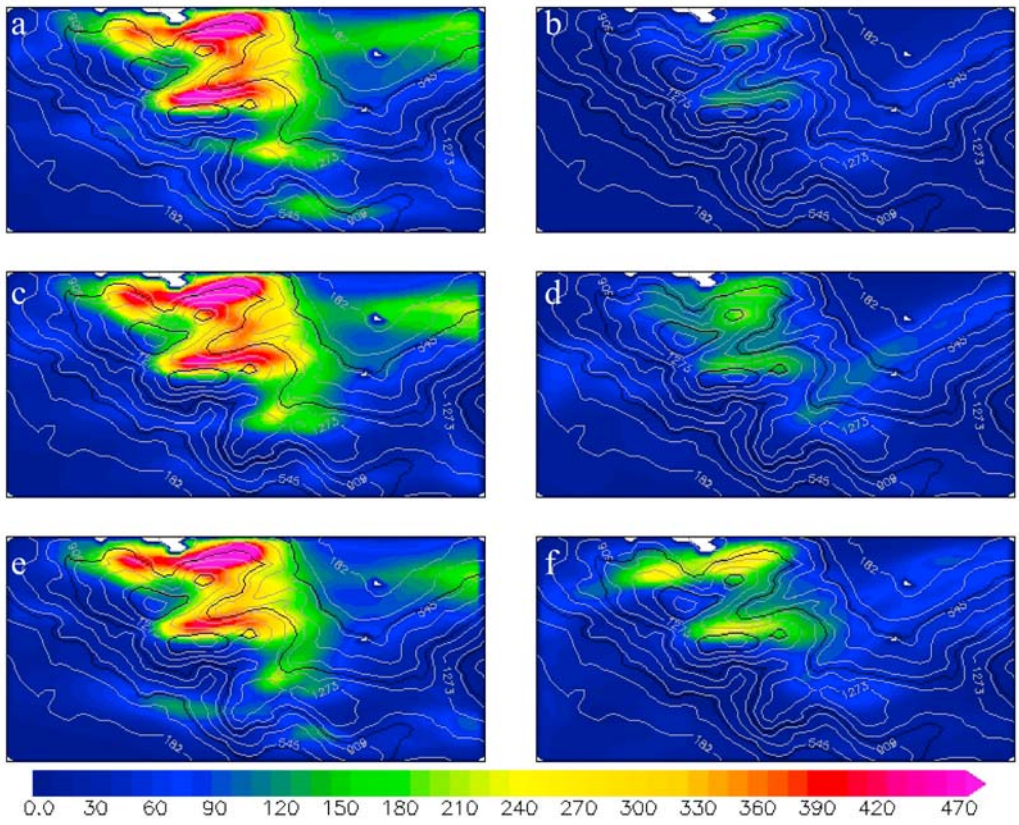

Figure 2. Simulated precipitation (mm) over the inner 1 km spatial resolution domain over the simulation period for six different model runs to assess the importance of special radiosondes: (a) F_SPECIAL run, (b) F_STANDARD run, (c) C_SPECIAL_ATM run, (d) C_STANDARD_ATM run, (e) D_SPECIAL run, and (f) D_STANDARD run.

3.2.1. Precipitation Comparisons

[23] The C_SPECIAL_ATM model simulated an average of 99.9 mm of precipitation (standard error (SE) = 2.2 mm; SE = $\frac{\sigma}{\sqrt{N}}$) for the high-resolution (grid spacing = 1 km) remote inner domain whereas the C_STANDARD_ATM model simulated 46.0 mm (SE = 0.8 mm) of precipitation (Table 2). The differences were statistically significant at $\alpha = 0.05$ using a two-tailed t-test with unequal variances (heteroscedastic t-test). For the outer coarser grid land areas (grid spacing = 4 km) similarly, C_SPECIAL_ATM model simulated an average of 41.9 mm (SE = 1.8 mm) precipitation and C_STANDARD_ATM model simulated 33.3 mm (SE = 1.0 mm) precipitation and the differences were statistically significant at $\alpha = 0.05$ using a two-tailed t-test with unequal variances assumed. $\varepsilon_{C,Atm}$ for precipitation would thus be −53.8 mm for the inner domain (Table 3) whereas for the outer coarser domain it would have been −8.5 mm. The effect of deforestation simulated using standard atmospheric data sets for the inner domain (i.e., $\Delta_{F\rightarrow C}$ and $\Delta_{C\rightarrow D}$) was 17.1 mm and 7.0 mm, respectively. Both results are statistically significant at $\alpha = 0.05$ using a one-tailed t-test with unequal variances. On the contrary, the effect of deforestation simulated using special atmospheric data sets (i.e., $\Delta^*_{F\rightarrow C}$ and $\Delta^*_{C\rightarrow D}$) were −5.0 mm and −9.0 mm, respectively, and these were also statistically significant at $\alpha = 0.05$. Thus, simulations using standard atmospheric data sets suggest that deforestation increases precipitation whereas simulations using special radiosondes suggest that deforestation leads to precipitation decreases, and both results are statistically significant.

[24] Spatially the "SPECIAL" and "STANDARD" runs gave strikingly different precipitation patterns over the high-resolution domain (Figure 2). In all the simulations, precipitation increased with elevation and on the windward Atlantic slopes. However, in the "SPECIAL" simulations, precipitation decreased with deforestation in the montane regions, while for the "STANDARD" runs they increased with deforestation. The simulated precipitation amount was also very different. "SPECIAL" runs simulated 250 mm to greater than 450 mm (increasing with elevation) on the windward Atlantic slopes, whereas the "STANDARD" runs simulated 100 mm to 300 mm (increasing with elevation) of precipitation. Over the outer model domain a similar pattern of precipitation differences (Figure 3) between the "SPECIAL" and "STANDARD" simulations for forested, current, and deforested land use scenarios were simulated. Precipitation increased with elevation over the windward Atlantic slopes of the mountain ranges that divide Costa Rica into Atlantic and Pacific sides for both types of simulations, but for the "STANDARD" runs, precipitation increased with deforestation and for the "SPECIAL" runs they decreased with deforestation. Note that the C_SPECIAL_ATM run was shown to simulate precipitation more accurately with lower RMSE of 26.8 mm

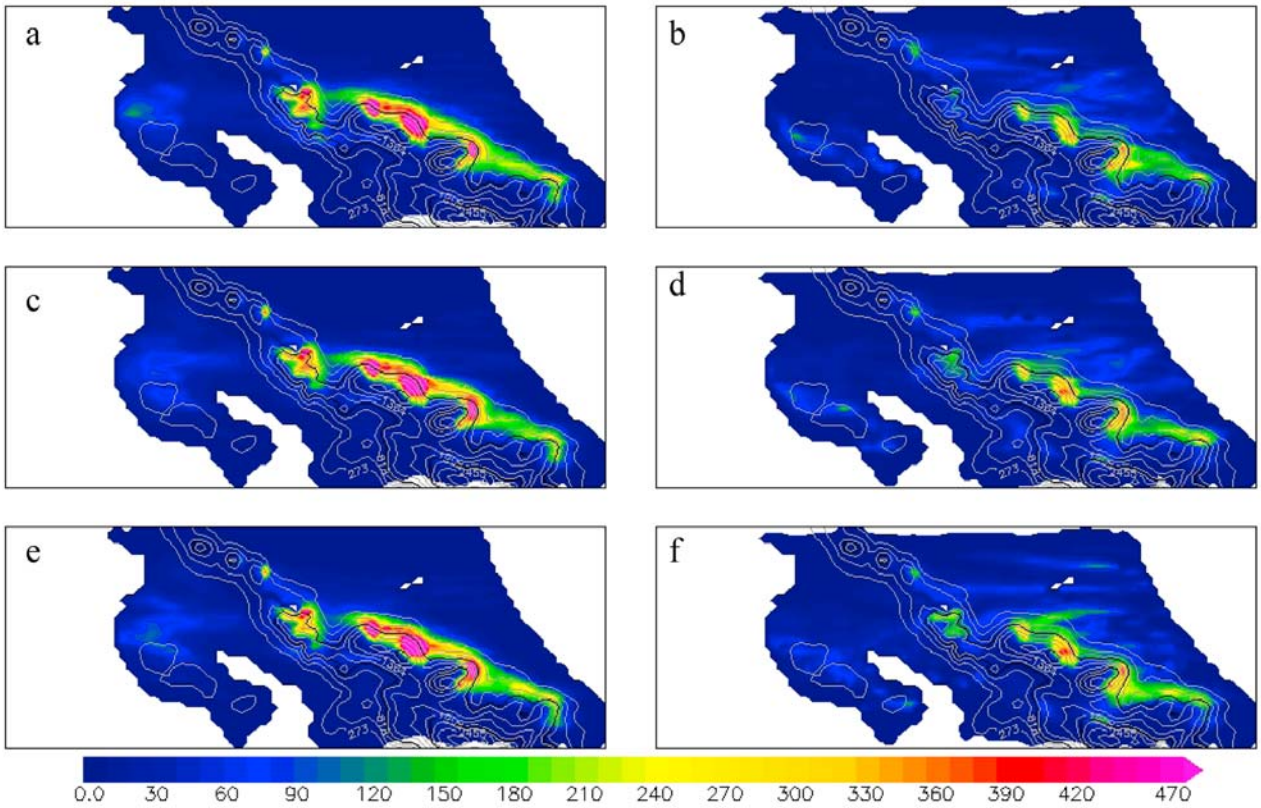

Figure 3. Simulated precipitation (mm) over the outer grid over the simulation period for six different models to estimate the importance of special radiosondes: (a) F_SPECIAL run, (b) F_STANDARD run, (c) C_SPECIAL_ATM run, (d) C_STANDARD_ATM run, (e) D_SPECIAL run, and (f) D_STANDARD run.

whereas C_STANDARD_ATM had a larger RMSE of 35.1 mm in section 3.1. Thus, a decrease in precipitation ($\Delta^*_{F\rightarrow C}$ and $\Delta^*_{C\rightarrow D}$) with deforestation is likely to be accurate for this location. Indeed previous studies have shown decrease in cloud cover with deforestation over this region [*Lawton et al.*, 2001; *Nair et al.*, 2003; *Ray et al.*, 2006a].

[25] Over the common remnant forest locations (i.e., those locations that are forested even in the deforested simulation scenario), and deforested locations (locations that are deforested in the deforestation land use scenario), precipitation $\varepsilon_{C,Atm}$, $\Delta_{F\rightarrow C}$ and $\Delta_{C\rightarrow D}$ was generally along similar lines of increases with deforestation for ''STANDARD'' model runs and decreases in precipitation with deforestation for ''SPECIAL'' runs (Table 3).

3.2.2. Surface Air Temperature Comparisons

[26] The 1400 LT averaged 2 m air temperature was 18.7°C for simulations using C_SPECIAL_ATM model but 23.0°C using the C_STANDARD_ATM model giving a $\varepsilon_{C,Atm}$ of 4.3°C for the high-resolution inner domain. $\Delta_{F\rightarrow C}$ was 2.4°C and $\Delta_{C\rightarrow D}$ was 0.4°C, implying that deforestation increases 2 m air temperature and additional deforestation further increases the 2 m air temperature. Results from simulations that used the special radiosondes were correspondingly 1.5°C and 0.4°C. Over remnant forest locations the results were similar but the magnitude of the values was lower. $\varepsilon_{C,Atm}$ was 2.9, $\Delta_{F\rightarrow C}$ was 0.3 but $\Delta_{F\rightarrow C}$ was 0.2; $\Delta_{C\rightarrow D}$ was 0.4 but $\Delta^*_{C\rightarrow D}$ was 0.2. Over the projected future locations of deforestation, the values were higher but results were similar. Similar results were also found at the other two peak daytime periods of 1500 and 1600 LT (Table 3).

[27] The diurnal variations of temperature averaged over the simulation period for the high-resolution inner domain show that during early morning and late evening hours the ''STANDARD'' and ''SPECIAL'' simulations varied by 1°C to 3°C between any two land use conditions (Figure 4). For example the ''STANDARD'' forested simulations had higher 2 m air temperatures than the ''SPECIAL'' forested simulation. The same was true for the current land use and for the projected future land use condition. However, during peak daytime hours the differences were as large as 6°C between identical land use conditions simply owing to whether the simulations used special radiosondes or not. Values were always higher for the ''STANDARD'' runs. Over the remnant cloud forest regions ''STANDARD'' runs simulated higher 2 m air temperatures for all three land use conditions compared to the ''SPECIAL'' runs that had lower 2 m air temperature for all three land use conditions. Over deforested regions the results were similar to the results found from simulations for the entire domain. The diurnal temperature variations show that while conclusions from ''STANDARD'' simulations would be similar to those simulations using special radiosondes, the actual magnitude of the temperature associated with each land use category would be quite different. In general, the ''STANDARD'' runs would suggest

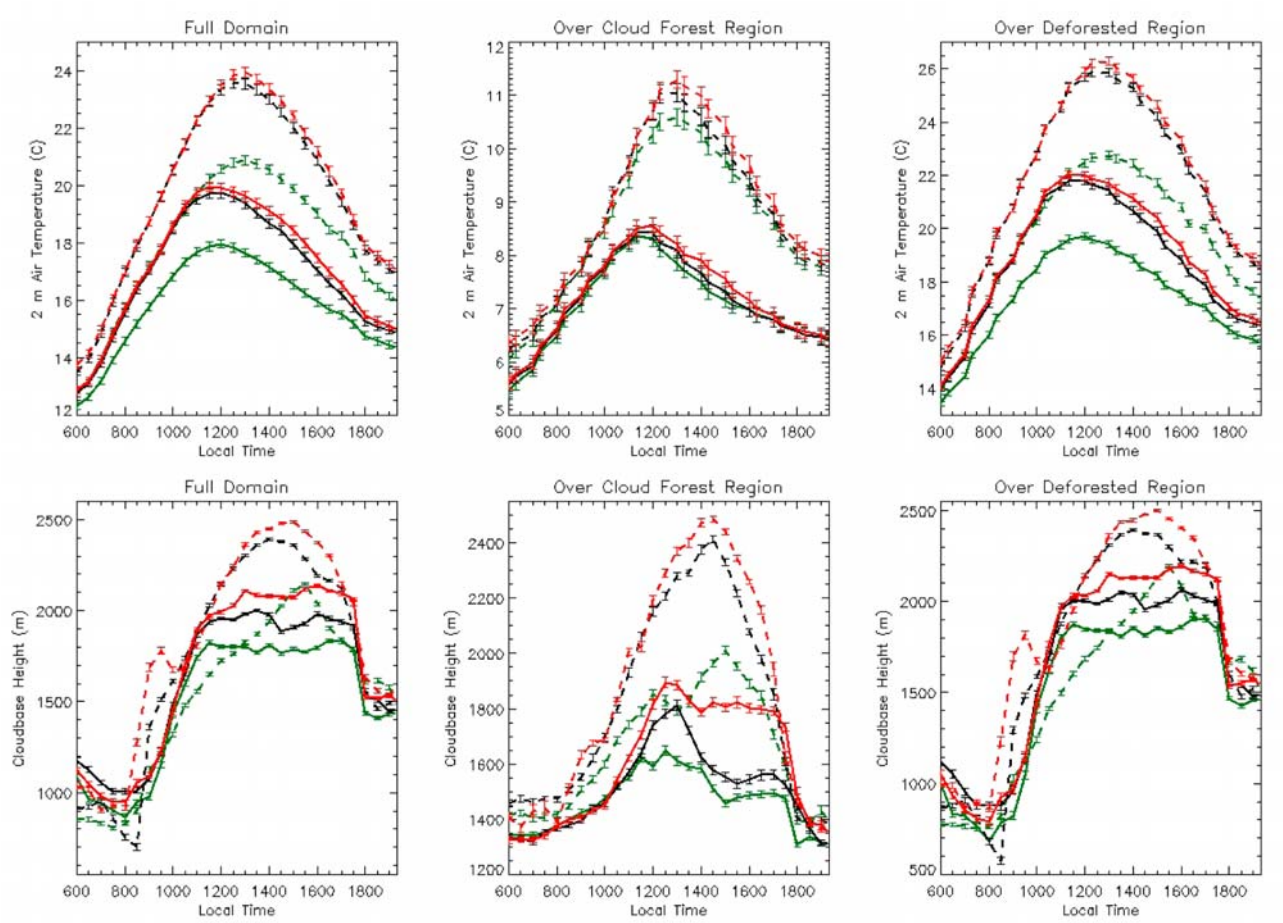

Figure 4. Impact of atmospheric information on simulating (top) 2 m air temperature and (bottom) cloud base heights. Solid lines are associated with simulations done with special radiosondes, whereas dashed lines are for simulations done with standard atmospheric information. Green denotes pristine/forest conditions, black denotes current conditions, and red denotes future deforested conditions. The error bars are associated with the standard error in each case.

that 2 m air temperatures are higher for each land use condition compared to the corresponding "SPECIAL" simulations.

3.2.3. Cloud Base Height Comparisons

[28] We computed cloud base height statistics because previous studies in this region concluded that land use changes [e.g., *Lawton et al.*, 2001; *Nair et al.*, 2003; *Ray et al.*, 2006a] or sea surface temperature rise [e.g., *Pounds et al.*, 1999; *Still et al.*, 1999; *Karmalkar et al.*, 2008] can impact cloud base heights and the sustainability of the endemic biodiversity at Monteverde. Our results show that cloud base heights computed using a regional-scale model would be highly sensitive to atmospheric information provided to it (Table 3). At 1500 LT for instance, $\varepsilon_{C,Atm}$ was 449.2 m. $\Delta_{F\rightarrow C}$ and $\Delta^*_{F\rightarrow C}$ were 249 m and 120.6 m. Note that the differences taken in both these cases are the same, that is, the difference in cloud base heights between current and forested land use conditions. The only difference being atmospheric information suggests that an additional cloud base height increase of 128.3 m would have been predicted simply from the usage of the "STANDARD" atmospheric information. Similarly, $\Delta_{C\rightarrow D}$ and $\Delta^*_{C\rightarrow D}$ were 128.1 m and 163.1 m at 1500 LT. Thus the diurnal variations in cloud base height over the remnant forest locations are also sensitive to the type of atmospheric information used in the simulations. "STANDARD" atmospheric information suggests cloud base height of even 2400 m at peak day time for current conditions. On the contrary, C_SPECIAL_ATM simulations suggest an increase in cloud base height from around 1600 m (corresponding to forested conditions) to peak values of around 1800 m (for current conditions). This corresponds well with the observed anuran population crashes, an increase in the upper elevation of bird ranges [*Lawton et al.*, 2001] at the Monteverde cloud forest preserve. On the contrary "STANDARD" runs suggest that cloud base heights have risen to above 1800 m between 1000 LT and 1700 LT; the entire peak daytime hours. Thus, according to the "STANDARD" simulations, the cloud bases generally did not intersect the mountains for the entire simulation period. This is not true and cloud base height observations from Monteverde [*Welch et al.*, 2008; *Nair et al.*, 2008] suggests that cloud base heights at 1030 LT varied between 1300 m to 1675 m for the identical time frame (1–15 March 2003) which is comparable to the approximately 1500 m average cloud base height simulated over the identical region using special radiosondes. The spatial variations of cloud base

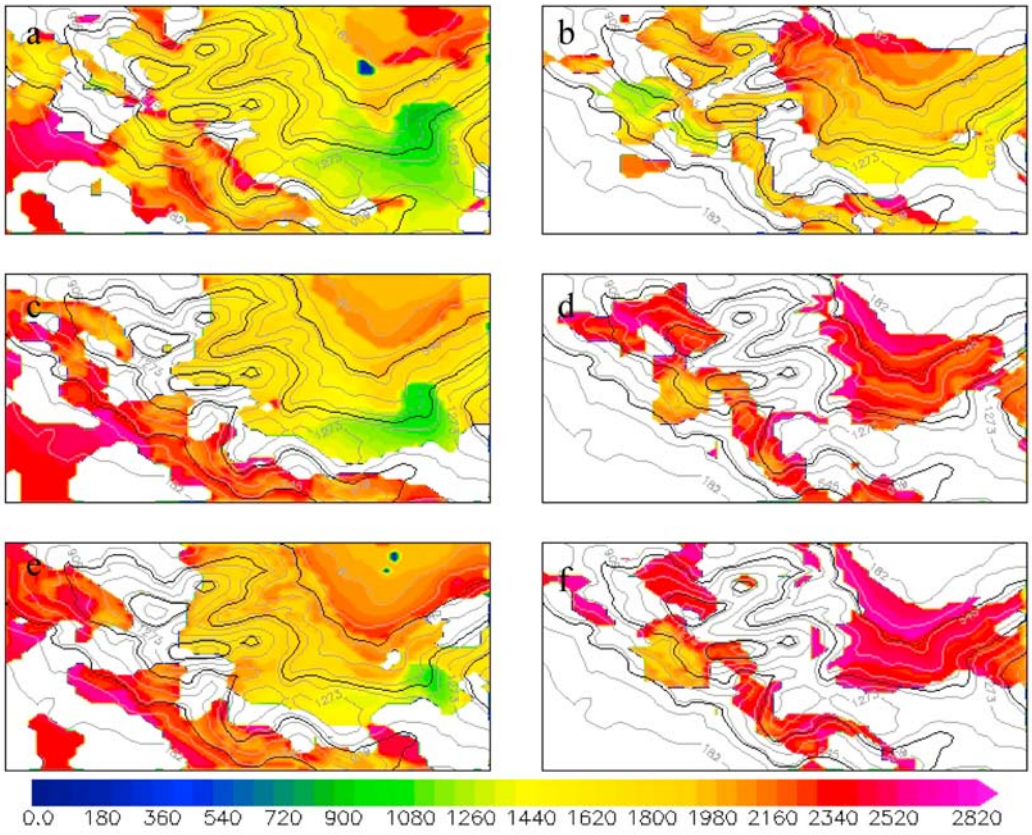

Figure 5. Average cloud base heights simulated over the inner high-resolution 1 km grid (m) (see Figure 1 for the geographic location of this inner grid) over the simulation period for six different models to estimate the importance of special radiosondes at 1400 LT: (a) F_SPECIAL run, (b) F_STANDARD run, (c) C_SPECIAL_ATM run, (d) C_STANDARD_ATM run, (e) D_SPECIAL run, and (f) D_STANDARD run. Clouds with bases above 3 km were not plotted.

heights at 1400 LT are shown in Figure 5. At other times (such as 1500 LT and 1600 LT) the results were similar. Cloud base heights increase with elevation as can be expected, but what is interesting is that (1) "STANDARD" simulations had fewer low-level clouds (clouds with bases at 2.75 km and below) for all three land use scenarios and (2) cloud base heights simulated over the montane regions tend to be at higher elevations and often more than the height of these mountains for the current land use, signifying that these regions must already be cloud-free. Using a higher cloud base height criteria, results were similar; that is, "STANDARD" simulations had fewer low-level clouds. This is not true as found by *Welch et al.* [2008] and *Nair et al.* [2008], signifying that the inaccuracies that occur in dynamic downscaling can provide misleading results unless RCMs are provided additional information such as provided in this study from special radiosondes.

3.3. The $\varepsilon_{C,Land}$ Compared With $\Delta^*_{F\rightarrow C}$ and $\Delta^*_{C\rightarrow D}$ Over Remote Cloud Forests

[29] Precipitation $\varepsilon_{C,Land}$ was −14.3 mm, whereas $\Delta_{F\rightarrow C}$ and $\Delta_{C\rightarrow D}$ were −19.3 mm and 5.3 mm over the entire inner remote domain, respectively. These values are comparable to $\Delta^*_{F\rightarrow C}$ and $\Delta^*_{C\rightarrow D}$ indicating lower gains in simulation accuracy by improving the current land cover information compared to improvements from additional atmospheric information. Over cloud forests these values were −40.1 mm, −35.4 mm, and 16.5 mm. The 2 m air temperature and cloud base height results were also along similar lines and not discussed further here. The question then arises regarding the relative role of uncertainties in the land use versus the atmospheric information. We used average wind speed variation with height (Figure 6) to estimate mass flushing rates (H. von Storch, personal communication, 2007). Strong winds cause large flushing rates while weak winds cause weak flushing rates and increase the residence time for land-atmosphere interactions. The memory of the initial conditions also decays more quickly for strong flushing rates. However, we found no such reason for the smaller importance of the land surface condition. We found that wind speed increased from around 5 m s^{-1} at low levels (on the order of 100 m) to around 10 m s^{-1} at the trade wind inversion level at approximately 3.5 km and then to 15 m s^{-1} higher up for the outer grid. Since the outer grid had a length of 400 km, a 5 m s^{-1} wind would have taken roughly 1 day to travel the entire length of the domain from the Atlantic coast to the Pacific coast providing sufficient time for exchanges with the land surface. Winds at the trade wind inversion level of course traveled faster and would have taken around 12 h to traverse the simulation domain. Thus, our results suggest that the quantitative agreement of regional weather model results with observations is less dependent on

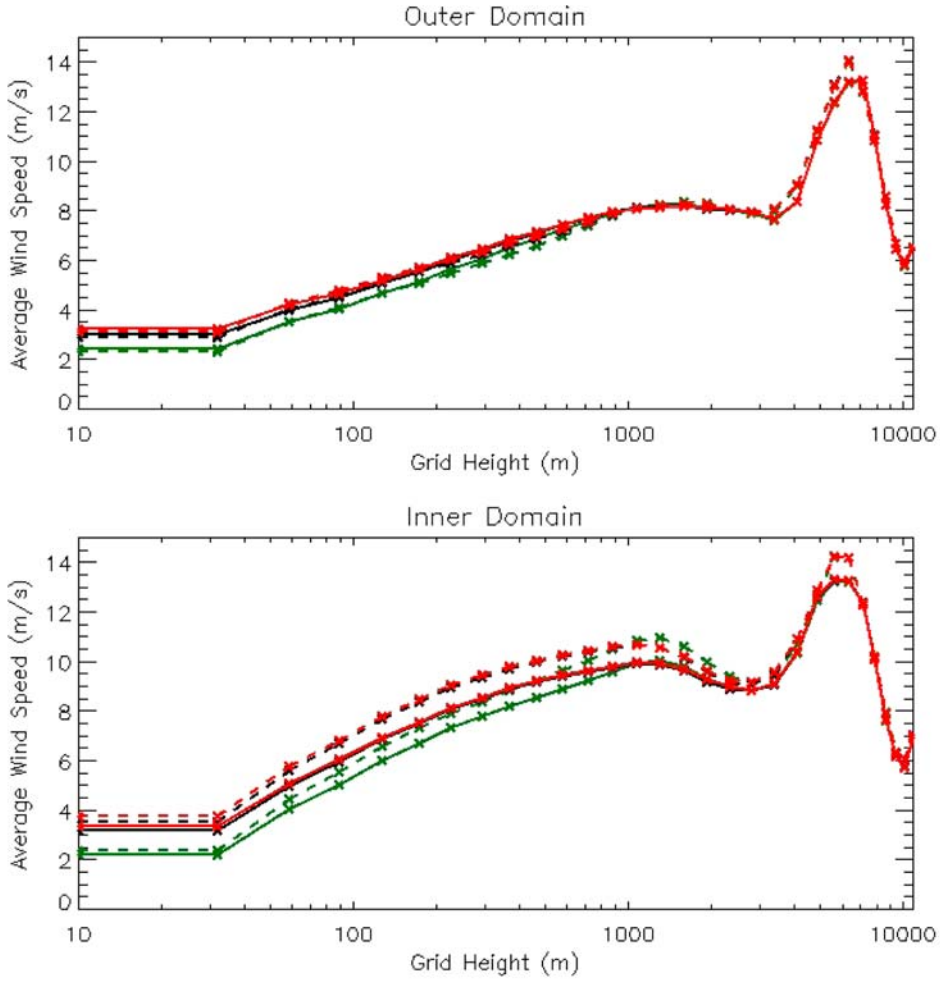

Figure 6. Variation of domain-averaged wind speed with height for all special atmosphere simulations for outer coarser domain and for the entire simulation time. The initial increase of wind speed with height decreases at around 3.5 km, and then it rapidly increases. This is associated with the trade wind inversion found in this region.

uncertainties in the land surface data than those in the atmospheric data for wind speeds typical of trade wind regimes.

4. Conclusions

[30] This analysis suggests that studies that deal with regional atmospheric effects of land use changes may have unknown uncertainties due to inaccuracies in their baseline simulations. We show that for the region around the Monteverde cloud forests in Costa Rica, simulations utilizing standard atmospheric data sets suggest increases in precipitation with lowland deforestation. However, with the added spatial resolution that is provided by special radiosondes, the results are just the opposite. The simulated 2 m air temperature and cloud base heights are also substantially different depending on the quality of atmospheric information provided to the model simulations. Thus the conclusions obtained in land cover change studies can be quite different because of the quality of atmospheric information provided to regional models.

[31] Our results are relevant to the four types of dynamic downscaling reported by *Castro et al.* [2005]. The time period of integration in this study corresponds to a type 1 downscaling in which we initialized our RCM with observed data and integrated it forward using data assimilation of observed data and lateral boundary conditions from the NCEP reanalysis. Our result showed that dynamic downscaling can provide misleading results unless RCMs are provided additional information. The results are also applicable to type 2 downscaling because the value-added (skill) of type 1 must be equal to or greater than type 2 since the insertion of initial conditions and continuous data assimilation provides a real-world constraint to the accuracy of the regional model. In fact, nudging is required in order to prevent the regional model from drifting away from the real world [*Rockel et al.*, 2008].

[32] We found $\varepsilon_{C,Atm}$ associated with precipitation (left-hand side of equations (11) and (13)) for the inner high-resolution domain was −53.6 mm. This was comparable in magnitude to the effects of deforestation (i.e., the signal being measured) using standard atmospheric data sets (i.e., $\Delta_{F\rightarrow C}$ and $\Delta_{C\rightarrow D}$, the right-hand side of equations (11) and (13),

respectively) and was 17.1 mm and 7.0 mm. Moreover, the impacts on precipitation due to deforestation simulated using the special atmospheric data sets (i.e., $\Delta^*_{F\rightarrow C}$ and $\Delta^*_{C\rightarrow D}$) were −5.1 mm and −9.0 mm, respectively, which was opposite in sign to those simulated using the "STANDARD" data set thereby suggesting that simulations using "STANDARD" atmospheric data sets are not only incorrect but can also provide misleading results; in this case that deforestation leads to increases in precipitation. The "STANDARD" atmospheric simulations were however wetter at the gauges but drier overall.

[33] The simulated diurnal variation in temperature by the "STANDARD" and "SPECIAL" simulations both show that deforestation leads to increases in 2 m air temperature. However, the "STANDARD" runs suggest significantly higher temperatures in comparison to the "SPECIAL" runs. Similarly, cloud base heights were significantly higher during the peak daytime for the "STANDARD" simulations and not found in actual observations for identical times [*Welch et al.*, 2008; *Nair et al.*, 2008]. The mass flushing similarly was higher for the "STANDARD" simulations compared to the "SPECIAL" simulations.

[34] Our results show that RCMs are strongly dependent on the lateral boundary conditions (and nudging) from the GCM (or reanalysis). When the RCMs are integrated far enough into the future such that their initial values are forgotten, as shown by *Castro et al.* [2005] and *Rockel et al.* [2008], the RCMs cannot add value (skill) with respect to atmospheric features that are resolved within the parent GCM (or reanalysis). Also, the regional climate results are so strongly controlled by the larger scale that they cannot correct for errors that occur within the larger-scale global climate prediction [*Chase et al.*, 2003; *Castro et al.*, 2005; *Lo et al.*, 2008]. What we show in this paper is that the accuracy of even type 1 downscaling is degraded without sufficient data on the regional atmospheric structure and these have important implications for land use change impact studies. The findings have implications not only for land cover change studies but also for future climate change predictions such as planned in the Fifth IPCC assessments, since type 3 and 4 downscaling [*Castro et al.*, 2005] must have even less value-added (skill) than type 1 and 2 downscaling.

[35] **Acknowledgments.** R. A. Pielke Sr. was supported in this study through the University of Colorado in Boulder (CIRES/ATOC). D. Niyogi benefited in part from the DOE ARM Program (08ER64674; Rick Petty and Kiran Alapaty), NSF CAREER-0847472 (Liming Zhou and J. Fein), and NASA Terrestrial Hydrology Program (Jared Entin). U.S. Nair was supported in this study by the National Aeronautics and Space Administration (NASA) grant NNS06AA588. We thank Dallas Staley for editorial support. John W. Nielson-Gammon and an anonymous reviewer are acknowledged for helpful comments that led to a significant improvement in the quality of our manuscript.

References

Alapaty, K., D. Niyogi, F. Chen, P. Pyle, A. Chandrasekar, and N. Seaman (2008), Development of the flux-adjusting surface data assimilation system for mesoscale models, *J. Appl. Meteorol. Climatol.*, *47*, 2331–2350, doi:10.1175/2008JAMC1831.1.

Alfieri, J., D. S. Niyogi, M. A. LeMone, F. Chen, and S. Fall (2007), A simple reclassification method for correcting uncertainty in land use/land cover data sets used with land surface models, *Pure Appl. Geophys.*, *164*, 1789–1809, doi:10.1007/s00024-007-0241-4.

Baidya Roy, S., and R. Avissar (2002), Impact of land use/land cover change on regional hydrometeorology in Amazonia, *J. Geophys. Res.*, *107*(D20), 8037, doi:10.1029/2000JD000266.

Castro, C. L., R. A. Pielke Sr., and G. Leoncini (2005), Dynamical downscaling: Assessment of value retained and added using the Regional Atmospheric Modeling System (RAMS), *J. Geophys. Res.*, *110*, D05108, doi:10.1029/2004JD004721.

Chase, T. N., R. A. Pielke Sr., and C. Castro (2003), Are present day climate simulations accurate enough for reliable regional downscaling?, *Water Resour. Update*, *124*, 26–34.

Chiew, F. H. S., and T. A. McMahon (2002), Modelling the impacts of climate change on Australian streamflow, *Hydrol. Processes*, *16*(6), 1235–1245, doi:10.1002/hyp.1059.

Douglas, E. M., A. Beltrán-Przekurat, D. S. Niyogi, R. A. Pielke Sr., and C. J. Vörösmarty (2009), The impact of agricultural intensification and irrigation on land-atmosphere interactions and Indian monsoon precipitation: A mesoscale modeling perspective, *Global Planet. Change*, *67*, 117–128, doi:10.1016/j.gloplacha.2008.12.007.

Fall, S., D. Niyogi, A. Gluhovsky, R. A. Pielke Sr., E. Kalnay, and G. Rochon (2009), Impacts of land use land cover on temperature trends over the continental United States: Assessment using the North American Regional Reanalysis, *Int. J. Climatol.*, doi:10.1002/joc.1996, in press.

Food and Agriculture Organization (1971), Soil map of the world, vol. II–X, scale 1:5,000,000, U.N. Educ. Sci. and Cult. Organ., Paris.

Ge, J., J. Qi, B. M. Lofgren, N. Moore, N. Torbick, and J. M. Olson (2007), Impacts of land use/cover classification accuracy on regional climate simulations, *J. Geophys. Res.*, *112*, D05107, doi:10.1029/2006JD007404.

Hansen, M. C., R. S. DeFries, J. R. G. Townshend, and R. Sohlberg (2000), Global land cover classification at the 1 km spatial resolution using a classification tree approach, *Int. J. Remote Sens.*, *21*, 1331–1364, doi:10.1080/014311600210209.

Harrington, J. Y., and P. Q. Olsson (2001), A method for the parameterization of cloud optical properties in bulk and bin microphysical models: Implications for Arctic cloudy boundary layers, *Atmos. Res.*, *57*, 51–80, doi:10.1016/S0169-8095(00)00068-5.

Kalnay, E., et al. (1996), The NCEP/NCAR 40-year reanalysis project, *Bull. Am. Meteorol. Soc.*, *77*, 437–471, doi:10.1175/1520-0477(1996)077<0437:TNYRP>2.0.CO;2.

Karmalkar, A. V., R. S. Bradley, and H. F. Diaz (2008), Climate change scenario for Costa Rican montane forests, *Geophys. Res. Lett.*, *35*, L11702, doi:10.1029/2008GL033940.

Kishtawal, C. M., D. Niyogi, M. Tewari, R. A. Pielke Sr., and M. Shepherd (2010), Urbanization signature in the observed heavy rainfall climatology over India, *Int. J. Climatol.*, doi:10.1002/joc.2044, in press.

Lawton, R. O., U. S. Nair, R. A. Pielke Sr., and R. M. Welch (2001), Climatic impact of tropical lowland deforestation on nearby montane cloud forests, *Science*, *294*, 584–587.

Lo, J. C.-F., Z.-L. Yang, and R. A. Pielke Sr. (2008), Assessment of three dynamical climate downscaling methods using the Weather Research and Forecasting (WRF) model, *J. Geophys. Res.*, *113*, D09112, doi:10.1029/2007JD009216.

Marshall, C. H., Jr., R. A. Pielke Sr., and L. T. Steyaert (2003), Crop freezes and land-use change in Florida, *Nature*, *426*, 29–30, doi:10.1038/426029a.

Marshall, C. H., Jr., R. A. Pielke Sr., L. T. Steyaert, and D. A. Willard (2004), The impact of anthropogenic land-cover change on the Florida peninsula sea breezes and warm season sensible weather, *Mon. Weather Rev.*, *132*, 28–52, doi:10.1175/1520-0493(2004)132<0028:TIOALC>2.0.CO;2.

Mellor, G. L., and T. Yamada (1982), Development of a turbulence closure model for geophysical fluid problems, *Rev. Geophys.*, *20*, 851–875, doi:10.1029/RG020i004p00851.

Mesinger, F., et al. (2006), North American regional reanalysis, *Bull. Am. Meteorol. Soc.*, *87*, 343–360, doi:10.1175/BAMS-87-3-343.

Nair, U. S., R. O. Lawton, R. M. Welch, and R. A. Pielke Sr. (2003), Impact of land use on Costa Rican tropical montane cloud forests: Sensitivity of cumulus cloud field characteristics to lowland deforestation, *J. Geophys. Res.*, *108*(D7), 4206, doi:10.1029/2001JD001135.

Nair, U. S., D. K. Ray, J. Wang, S. A. Christopher, T. J. Lyons, R. M. Welch, and R. A. Pielke Sr. (2007), Observational estimates of radiative forcing due to land use change in southwest Australia, *J. Geophys. Res.*, *112*, D09117, doi:10.1029/2006JD007505.

Nair, U. S., S. Asefi, R. M. Welch, D. K. Ray, R. O. Lawton, V. S. Manoharan, M. Mulligan, T. L. Sever, D. Irwin, and A. Pounds (2008), Biogeography of tropical montane cloud forests. Part II: Mapping of orographic cloud immersion, *J. Appl. Meteorol. Climatol.*, *47*, 2183–2197, doi:10.1175/2007JAMC1819.1.

Niyogi, D., S. Raman, and K. Alapaty (1999), Uncertainty in specification of surface characteristics, Part 2: Hierarchy of interaction explicit statistical analysis, *Boundary Layer Meteorol.*, *91*, 341–366, doi:10.1023/A:1002023724201.

Niyogi, D., Y.-K. Xue, and S. Raman (2002), Hydrological land surface response in a tropical regime and a midlatitudinal regime, *J. Hydrometeorol.*, *3*, 39–56, doi:10.1175/1525-7541(2002)003<0039:HLSRIA>2.0.CO;2.

Niyogi, D., C. Kishtawal, S. Tripathi, and R. S. Govindaraju (2010), Observational evidence that agricultural intensification and land use change may be reducing the Indian summer monsoon rainfall, *Water Resour. Res.*, doi:10.1029/2008WR007082, in press.

Pielke, R. A., Sr. (2001), Influence of the spatial distribution of vegetation and soils on the prediction of cumulus convective rainfall, *Rev. Geophys.*, *39*, 151–177, doi:10.1029/1999RG000072.

Pielke, R. A., et al. (1992), A comprehensive meteorological modeling system: RAMS, *Meteorol. Atmos. Phys.*, *49*, 69–91, doi:10.1007/BF01025401.

Pielke, R. A., Sr., J. Adegoke, A. Beltran-Przekurat, C. A. Hiemstra, J. Lin, U. S. Nair, D. Niyogi, and T. E. Nobis (2007), An overview of regional land use and land cover impacts on rainfall, *Tellus Ser. B*, *59*, 587–601, doi:10.1111/j.1600-0889.2007.00251.x.

Pounds, A. J., M. P. L. Fogden, and J. H. Campbell (1999), Biological response to climate change on a tropical mountain, *Nature*, *398*, 611–615, doi:10.1038/19297.

Ramankutty, N., and J. A. Foley (1999), Estimating historical changes in global land cover: Croplands from 1700 to 1992, *Global Biogeochem. Cycles*, *13*, 997–1027, doi:10.1029/1999GB900046.

Ray, D. K., and B. C. Pijanowski (2010), A backcast land use change model to generate past land use maps: Application and validation at the Muskegon River watershed of Michigan, USA, *J. Land Use Sci.*, *5*(1), 1–29, doi:10.1080/17474230903150799.

Ray, D. K., U. S. Nair, R. M. Welch, Q. Han, J. Zeng, W. Su, T. Kikuchi, and T. J. Lyons (2003), Effects of land use in Southwest Australia: 1. Observations of cumulus cloudiness and energy fluxes, *J. Geophys. Res.*, *108*(D14), 4414, doi:10.1029/2002JD002654.

Ray, D. K., U. S. Nair, R. O. Lawton, R. M. Welch, and R. A. Pielke Sr. (2006a), Impact of land use on Costa Rican tropical montane cloud forests: Sensitivity of orographic cloud formation to deforestation in the plains, *J. Geophys. Res.*, *111*, D02108, doi:10.1029/2005JD006096.

Ray, D. K., R. M. Welch, R. O. Lawton, and U. S. Nair (2006b), Dry season clouds and rainfall in northern Central America: Implications for the Mesoamerican Biological Corridor, *Global Planet. Change*, *54*, 150–162, doi:10.1016/j.gloplacha.2005.09.004.

Ray, D. K., R. A. Pielke Sr., U. S. Nair, R. M. Welch, and R. O. Lawton (2009), Importance of land use versus atmospheric information verified from cloud simulations from a frontier region in Costa Rica, *J. Geophys. Res.*, *114*, D08113, doi:10.1029/2007JD009565.

Rockel, B., C. L. Castro, R. A. Pielke Sr., H. von Storch, and G. Leoncini (2008), Dynamical downscaling: Assessment of model system dependent retained and added variability for two different regional climate models, *J. Geophys. Res.*, *113*, D21107, doi:10.1029/2007JD009461.

Scibek, J., and D. M. Allen (2006), Modeled impacts of predicted climate change on recharge and groundwater levels, *Water Resour. Res.*, *42*, W11405, doi:10.1029/2005WR004742.

Still, C. J., P. N. Foster, and S. H. Schneider (1999), Simulating the effects of climate change on tropical montane cloud forests, *Nature*, *389*, 608–610.

Taylor, C. M., and R. J. Ellis (2006), Satellite detection of soil moisture impacts on convection at the mesoscale, *Geophys. Res. Lett.*, *33*, L03404, doi:10.1029/2005GL025252.

Tucci, C. E. M., R. T. Clarke, W. Collischonn, P. L. da Silva Dias, and G. S. de Oliveira (2003), Long-term flow forecasts based on climate and hydrologic modeling: Uruguay River basin, *Water Resour. Res.*, *39*(7), 1181, doi:10.1029/2003WR002074.

Visbeck, M. (2008), From climate assessment to climate services, *Nat. Geosci.*, *1*, 2–3, doi:10.1038/ngeo.2007.55.

Welch, R. M., S. Asefi, J. Zeng, U. S. Nair, Q. Han, R. O. Lawton, D. K. Ray, and V. S. Manoharan (2008), Biogeography of tropical montane cloud forests. Part 1: Remote sensing of cloud base heights, *J. Appl. Meteorol. Climatol.*, *47*, 960–975, doi:10.1175/2007JAMC1668.1.

Wu, Y., U. S. Nair, R. A. Pielke Sr., R.T. McNider, S. A. Christopher, and V. G. Anantharaj (2009), Impact of land surface heterogeneity on mesoscale atmospheric dispersion, *Boundary Layer Meteorol.*, *133*, 367–389, doi:10.1007/s10546-009-9415-1.

U. S. Nair, Earth System Science Center, National Space Science and Technology Center, University of Alabama at Huntsville, Huntsville, AL 35805, USA.

D. Niyogi, Department of Agronomy, Purdue University, West Lafayette, IN 47907, USA.

R. A. Pielke Sr., Cooperative Institute for Research in Environmental Sciences, University of Colorado at Boulder, Boulder, CO 80309, USA.

D. K. Ray, Institute on the Environment, University of Minnesota–Twin Cities, Saint Paul, MN 55108, USA. (dray@umn.edu)